Rapid shifts in methanotrophic bacterial communities mitigate methane emissions from a tropical hydropower reservoir and its downstream river

AUTHORS

Paula CJ Reis [1]*

Clara Ruiz-González [2]

Sophie Crevecoeur [3]

Cynthia Soued [1]

Yves T Prairie [1]

[1] Département des Sciences Biologiques, Groupe de Recherche Interuniversitaire en Limnologie, Université du Québec à Montréal, Montréal, QC, Canada.

[2] Departament de Biologia Marina i Oceanografia, Institut de Ciències del Mar (ICM-CSIC), Barcelona, Spain.

[3] Canada Centre for Inland Waters, Water Science and Technology Branch - Watershed Hydrology and Ecology Research Division, Environment and Climate Change Canada, Burlington, ON, Canada.

* corresponding author: paulacjr@gmail.com.

Postal address: 141 Avenue du Président-Kennedy, Montréal, QC H2X 1Y4 CANADA

HIGHLIGHTS

- Methane-oxidizing bacteria (MOB) can reach high abundances in reservoirs.
- Inflowing MOB communities are restructured along a hydropower complex.
- Methane dynamics can be accompanied by rapid shifts in MOB communities.

ABSTRACT

Methane-oxidizing bacteria (MOB) present in the water column mitigate methane (CH_4) emissions from hydropower complexes to the atmosphere. By creating a discontinuity in rivers, dams cause large environmental variations, including in CH_4 and oxygen concentrations, between upstream, reservoir, and downstream segments. Although highest freshwater methanotrophic activity is often detected at low oxygen concentrations, CH_4 oxidation in well-oxygenated downstream rivers below dams has also been reported. Here we combined DNA and RNA high-throughput sequencing with microscopic enumeration (by CARD-FISH) and biogeochemical data to investigate the abundance, composition, and potential activity of MOB taxa from upstream to downstream waters in the tropical hydropower complex Batang Ai (Malaysia). High relative abundance of MOB (up to 61% in 16S rRNA sequences and 19% in cell counts) and enrichment of stable isotopic signatures of CH_4 (up to 0‰) were detected in the hypoxic hypolimnion of the reservoir and in the outflowing downstream river. MOB community shifts along the river-reservoir system reflected environmental sorting of taxa and an interrupted hydrologic connectivity in which downstream MOB communities resembled reservoir's hypolimnetic communities but differed from upstream and surface reservoir communities. In downstream waters, CH_4 oxidation was accompanied by fast cell growth of

particular MOB taxa. Therefore, our results suggest that rapid shifts in active MOB communities allow the mitigation of CH_4 emissions from different zones of hydropower complexes, including in quickly re-oxygenated rivers downstream of dams.

Keywords: methanotrophic bacteria, methane, reservoir, hydropower, tropical.

1. INTRODUCTION

The damming of rivers for hydropower generation can alter the carbon biogeochemical cycling across the entire river network through increased water residence time, water column stratification, and anoxic conditions in sediments and bottom waters (Tremblay et al., 2005). These changes can affect the place and time in which carbon is processed and mineralized, ultimately affecting the dynamics of greenhouse gases in these systems (Prairie et al., 2017). For instance, reservoirs are important CH_4 sources to the atmosphere, emitting relevant amounts of CH_4 at a global scale, although current estimates of their significance vary widely (3-14 TgC-CH_4 $year^{-1}$; St. Louis et al. 2000; Barros et al. 2011; Deemer et al. 2016). Thus, a better understanding of the processes controlling CH_4 emissions from hydropower reservoirs could contribute to more accurate estimations as well as predictions of future reservoirs' CH_4 emissions.

A particularly important process regulating CH_4 emissions from reservoirs is CH_4 oxidation performed by methane-oxidizing bacteria (MOB, here also referred to as methanotrophs) present in the water column. These bacteria can oxidize a large fraction of the CH_4 produced in freshwaters before it reaches the atmosphere, strongly mitigating the carbon

footprint of hydropower impoundments (e.g. Guérin and Abril, 2007; Itoh et al., 2015). MOB comprise an ecologically diverse polyphyletic group of bacteria mostly distributed within the Classes Gammaproteobacteria (Gamma-MOB) and Alphaproteobacteria (Alpha-MOB), but also in the phyla NC10 and Verrucomicrobia (Kalyuzhnaya et al., 2019). These different groups show distinct environmental niches and tolerances, metabolic capacities, and life strategies (Dunfield et al., 2007; Ettwig et al., 2010; Hanson and Hanson, 1996; Ho et al., 2013) that are related to gradients in environmental variables in freshwaters such as O_2 and CH_4 concentrations, temperature, and pH (Borrel et al., 2011; Conrad, 2007; Crevecoeur et al., 2019; Reis et al., 2020) and that can lead to different contributions to the overall CH_4 oxidation rate (Reis et al. 2020). Dams constitute a discontinuity in river systems causing large environmental variations between upstream, reservoir, and downstream segments, which have been shown to alter the structure of river bacterioplankton communities (Dumestre et al., 2001; Ruiz-González et al., 2015b, 2013). Similarly, thermal stratification within reservoirs can generate large environmental changes between water column layers leading to a rearrangement of the inflowing bacterial communities (Dumestre et al., 1999). Such environmental variations could thus trigger the establishment of distinct MOB communities and associated activity between zones within hydropower complexes, thereby influencing the role of MOB taxa in mitigating CH_4 emissions. For instance, it has been shown that while Gamma-MOB dominates overall CH_4 oxidation in temperate lakes (Oswald et al., 2016; Reis et al., 2020; Rissanen et al., 2018), Alpha-MOB may be important players particularly in well-oxygenated waters (Reis et al., 2020; Zigah et al., 2015).

Besides CH_4 emissions from the surface of reservoirs, hydropower turbines often draw water from CH_4-rich hypolimnia, and their CH_4 content is then released either immediately at the outflow (degassing) or at the surface of the downstream river (downstream diffusion). Due to strong water column stratification, these two downstream emission pathways often contribute the most to the greenhouse gas footprint of reservoirs in tropical regions (Abril et al., 2005; Guérin et al., 2006; Kemenes et al., 2007; Soued and Prairie, 2020). Freshwater methanotrophs appear to be most active at oxic-anoxic interfaces, with their activity being reduced at high dissolved O_2 concentrations (Rudd et al., 1974; Steinle et al., 2017; Thottathil et al., 2019). Therefore, one would expect a decrease in methanotrophic activity due to a rapid re-oxygenation of turbine outflowing waters. Interestingly, however, significant microbial CH_4 oxidation has been detected in rivers downstream of dams by means of CH_4 concentration, flux, and stable isotopes, comprising between 20 and 85% of the CH_4 loss in downstream reaches (Abril et al., 2005; Guérin and Abril, 2007; Kemenes et al., 2007; Soued and Prairie, 2020). However, it remains unknown whether the reported CH_4 oxidation in downstream waters is due to residual activity of MOB transported from the reservoir's hypolimnion, or alternatively, to shifts in methanotrophic communities once these microorganisms are exposed to well oxygenated conditions. Knowledge of the dynamics of MOB communities along the river-reservoir continuum can thus provide insights into the ecological mechanisms behind CH_4 oxidation and emissions from hydropower complexes.

Here we examine the dynamics of the MOB community in the tropical Batang Ai hydropower complex throughout its hydrological continuum, from the reservoir inflows to the downstream outflow. We used high-throughput sequencing of the 16S rRNA gene (DNA) and of

the 16S rRNA (RNA) to determine the diversity and potential activity of MOB taxa along this hydropower river-reservoir system, as well as catalyzed reporter deposition fluorescence in situ hybridization (CARD-FISH) to microscopically quantify the Alpha- and Gamma-MOB groups. We expected that the hydrologic disruption caused by the dam would lead to strong environmental sorting of upstream inflowing MOB taxa and that the change from hypoxic hypolimnetic waters to the rapidly re-oxygenated turbine outflowing waters would trigger the growth and activity of MOB taxa that may be responsible for the oxidation of CH_4 in downstream waters.

2. METHODS

2.1. Study site and sampling

The hydropower reservoir Batang Ai is located in the Borneo Island, Malaysia (1°09'36"N 111°54'00"E), in a tropical equatorial climate with year-round hot and humid rainy weather. The reservoir was created in 1985, by damming of the Batang Ai river and flooding of un-cleared tropical forest. It has a surface area of 68.4 km^2, a mean depth of 28 m and maximum depth of 72 m, and two major river inflows that flow into two reservoir branches (Fig. 1). The water residence time in the reservoir is approx. 11 months, but of only around 1 hour in the studied segments of the upstream and downstream rivers. The main basin of the reservoir is permanently stratified with the thermocline around 12 m depth, the oxycline between 12 and 20 m depth, and anoxic bottom waters. The reservoir is characterized by high water temperatures (31 °C at the surface and 24 °C at the bottom) around the year, and low concentrations of dissolved organic carbon (<1 mg L^{-1} on average), chlorophyll (surface mean: 1.3 µg L^{-1}), total phosphorus (surface mean: 5.9 µg L^{-1}), and total nitrogen (surface mean: 0.1

mg L^{-1}) (Soued and Prairie, 2020). In the main base of the reservoir, diffusive CH_4 emissions to the atmosphere are moderate, and most CH_4 is emitted downstream of the dam since the water intake for the turbines is located in the highly CH_4-rich hypolimnion (Soued and Prairie, 2020). Nevertheless, CH_4 oxidation in the first 19 km downstream of the dam has been shown to reduce further diffusive CH_4 emissions by roughly 20% (Soued and Prairie, 2020).

Two sampling campaigns were performed, one in April-May 2017 and another in February-March 2018, both showing similar inflow discharge rates, although the official rainy season happens between October and March. In each sampling campaign, samples for biogeochemical parameters and microbial community were collected with a peristaltic pump at 10 different sites and at different depths in the reservoir, covering the horizontal gradient (upstream, reservoir, and downstream sites – one at the power station and another at 2.7 Km further downstream) and the vertical stratification within the reservoir (mixed layer and oxic and hypoxic hypolimnion, with oxic and hypoxic being defined as O_2 > and < 2 mg L^{-1}, respectively) (Fig. 1). Vertical profiles of temperature, dissolved O_2 concentration, and pH were measured with a YSI multiparameter probe (Yellow Springs Instruments, OH, USA). Sampling depths for the microbial community (Table S1) were determined based on the temperature and O_2 profiles in order to cover the thermal stratification layers but also the different O_2 concentrations in the water column, given that the O_2 profiles revealed a variation in the oxygenation of stratified layers from one site to another. To capture the changes in CH_4 and methanotrophic communities from the hypolimnion of the reservoir until the downstream river, we used the closest available samples to the turbine water intake depth in both years (2017: site A, depth 20 m; 2018: site I, depth 24 m).

154

155 *2.2. CH_4 concentration, stable isotopic signature, and downstream CH_4 oxidation*

156 Measurements of dissolved CH_4 concentration and its stable isotopic signature ($\delta^{13}CH_4$)
157 were determined using the headspace technique in 60 mL gas-tight syringes followed by gas
158 chromatography (GC-8A/GC-2014, Shimadzu, Kyoto, Japan) and cavity ring down spectrometry
159 (G2201-i, Picarro Inc., CA, USA). The $\delta^{13}CH_4$ signature is a useful indicator of microbial CH_4
160 oxidation since the methane monooxygenase enzyme preferentially oxidizes ^{12}C-CH_4 over ^{13}C-
161 CH_4 leaving an enriched $\delta^{13}CH_4$ signature in the remaining CH_4 pool (Coleman et al., 1981).

162 In the downstream river, we calculated the fraction and amount of CH_4 oxidized based
163 on the evolution of CH_4 concentration and isotopic signature from the turbine water intake in
164 the reservoir (considered as the CH_4 source) until 2.7 km downstream of the dam, using model
165 developed in Soued and Prairie (2020).

166

167 *2.3. MOB community composition*

168 We used amplicon sequencing of the 16S rRNA gene (DNA) and the 16S rRNA (RNA) of
169 37 water samples to identify and determine the relative abundance of prokaryotes belonging to
170 methane-oxidizing bacteria (MOB) taxa. We then extracted the MOB taxa from the 16S rRNA
171 database to investigate the taxonomic composition of MOB assemblages and community
172 dynamics along the river-reservoir system. By sequencing the DNA, we aimed at evaluating the
173 presence of MOB taxa and their role in the total bacterial community independently of their
174 activity state, while by sequencing the RNA we aimed at assessing the contribution of MOB taxa
175 to the potentially protein synthesizing bacterial community (Blazewicz et al., 2013).

For each sample, between 400 and 700 mL of water were prefiltered through a 30 µm pore size mesh and then filtered through Durapore membrane filters (0.22 µm pore size, GVWP, Millipore). Filters were preserved in RNAlater (Invitrogen), stored at 4 °C overnight, and then stored at -80 °C before nucleic acids extraction. All samples were extracted with PowerWater RNeasy extraction kit (Qiagen) skipping the step for DNA digestion to recover both DNA and RNA from the same filter. PCR amplification of the 16S rRNA gene with primers 515F (5'-GTGCCAGCMGCCGCGGTAA-3') and 806R (5'-GGACTACHVGGGTWTCTAAT-3') was carried out in every sample and samples with PCR inhibition (detected by the lack of amplification of positive control added into samples) were cleaned with a DNA cleaning kit (Qiagen). After that, half of each sample (25 µL) was digested with a DNase Max kit (Qiagen) to get pure RNA which was verified by the lack of amplification of the 16S rRNA gene by PCR and gel electrophoresis. Finally, cDNA was produced from RNA using a reverse transcription kit (Qiagen). DNA and cDNA 16S amplicons were sequenced in GenomeQuebec following a pair-end approach using Illumina MiSeq platform.

Sequences were analysed using the dada2 pipeline v1.8 (Callahan et al., 2016) in R v3.5.1 (The R Core Team, 2019) and R Studio (RStudio, 2018). Read quality was inspected using quality profiles and both forward and reverse reads were trimmed to 245 nucleotides. Primers were also removed using trimLeft() function in dada2 (19 nucleotides in forward and 20 in reverse reads). The average number of reads per sample was 77,948 (range 7,399 – 115,142). An Amplicon Sequence Variant (ASV) table was produced following the dada2 pipeline with an additional step to collapse together sequences that are only different in length ('collapseNoMismatch()'), which minimizes false singletons. Taxonomy assignment was

198 performed until the Genus level with SILVA reference database v132 using dada2's
199 'assignTaxonomy' function. Briefly, the 'assignTaxonomy' function uses a naïve Bayesian
200 classifier to compare the query sequences to sequences with assigned taxonomy in a database
201 and then a bootstrapping approach to assess the confidence estimates for each assignment
202 (Wang et al., 2007). Sequences assigned to Archaea, eukaryotes, or chloroplast were removed.
203 The ASV table (17,050 ASVs) was then rarefied using the R package phyloseq v1.22.3 (Mcmurdie
204 and Holmes, 2013) at a minimum of 50,000 reads per sample – leading to the loss of two
205 samples – and normalized to proportions so that ASVs abundances are ratios from 0 to 1. The
206 final rarefied dataset contained a total of 14,323 ASVs. Then, the final ASV table was screened
207 for known methanotrophic bacterial taxa: Order Melthylococcales (Class
208 Gammaproteobacteria); genera *Methylocystis* and *Methylosinus* (Class Alphaproteobacteria,
209 Family Methylocystaceae); genera *Methylocella*, *Methylocapsa*, and *Methyloferula* (Class
210 Alphaproteobacteria, Family Beijerinckiaceae); genera *Methylacidiphilum* and
211 *Methylacidimicrobium* (Phylum Verrucomicrobia); and '*Ca.* Methylomirabilis oxyfera' and
212 putative methanotrophs within the Order Methylomirabilales (Candidate phylum NC10)
213 (Dunfield et al., 2007; Ettwig et al., 2010; Kalyuzhnaya et al., 2019; Knief, 2015). For abundant
214 MOB ASVs that could only be assigned at the Family level, we used the NCBI Nucleotide BLAST
215 tool (https://blast.ncbi.nlm.nih.gov/Blast.cgi) to identify to which taxa they showed closest
216 percent identity.
217
218 *2.4. Cell abundance of Proteobacterial MOB groups*

We determined the absolute abundance of MOB cells belonging to Alpha- and Gammaproteobacteria through Catalyzed Reporter Deposition-Fluorescence In Situ Hybridization (CARD-FISH). Only the subset of samples in which MOB sequences was higher than 1% of total 16S rRNA sequences (DNA or RNA) were analysed (n=20), which excluded all samples from the surface mixed layer of the reservoir (Table S1). Water samples for CARD-FISH were treated and analysed as described in Reis et al. (2020). Briefly, water samples (40 mL) were fixed overnight with buffered paraformaldehyde (PFA, 1% final concentration) and then 6 to 10 mL of sample were filtered through 0.2 µm polycarbonate filters (Millipore GTTP, 25 mm). Cells were attached with 0.1% agarose and permeabilized with lysozyme and achromopeptidase. Hybridization was carried out with specific probes designed for the detection of Alpha- and Gammaproteobacteria MOB (Table S2; Eller et al. 2001) overnight at 35°C in 40% formamide hybridization buffer. Both CARD-FISH positive and DAPI (4',6-diamidino-2-phenylindole staining) positive cells were quantified under an automated epifluorescence microscope at 630x magnification counting on average 50 (min-max: 36-55) quality-checked fields of view. Cell counts of Alpha- and Gamma-MOB (CARD-FISH) as well as those of total prokaryotic cells (DAPI) were determined using the ACME tool3 software (Zeder, 2014).

2.5. Statistical analyses

Statistical differences between means were tested using Welch's unequal variances t-test on the log data when necessary. Canonical Analyses of Principal Coordinates-CAP (Anderson and Willis, 2003) based on the Bray-Curtis distance of the relative abundances of MOB ASVs in a sample were used to investigate differences in the MOB community structure in DNA and RNA

241 and their environmental drivers across the sampled sites. We included temperature, pH, CH_4,
242 O_2 and dissolved organic carbon (DOC) concentrations as environmental variables in the model
243 because of their reported influence on freshwater MOB community composition or activity
244 (Borrel et al., 2011; Conrad, 2007; Crevecoeur et al., 2019; Reis et al., 2020; Thottathil et al.,
245 2018). All analyses were performed in R v3.5.1 (The R Core Team, 2019) and R studio (RStudio,
246 2018) and plots were produced using the packages ggplot2 3.1.0 (Wickham, 2016) and phyloseq
247 v1.22.3 (Mcmurdie and Holmes, 2013).
248

249 **3. RESULTS**

250 *3.1. CH_4, $\delta^{13}CH_4$, and O_2 dynamics*

251 CH_4 concentration, CH_4 stable isotopic signature, and dissolved O_2 concentration varied
252 largely both horizontally and vertically in Batang Ai (Figs. 2A-C, 3). In both sampling campaigns,
253 the highest CH_4 concentration was detected in the anoxic zone of the reservoir's hypolimnion,
254 followed by downstream and upstream waters (Figs. 2, 3). CH_4 concentration was highly
255 variable within the hypoxic hypolimnion, varying up to three orders of magnitude even within a
256 single profile (Figs. 2A, 3). This was caused by intense microbial CH_4 oxidation in the hypoxic
257 hypolimnion as indicated by enriched $\delta^{13}CH_4$ values measured in this layer throughout the
258 system (Fig. 2B) and in individual profiles (Fig. 3). In contrast, the $\delta^{13}CH_4$ in the oxic hypolimnion
259 and in the surface mixed layer, particularly in 2017, suggests less methanotrophic activity in
260 these layers (Figs. 2B, 3). O_2 concentrations were highest in upstream waters and in the
261 reservoir mixed layer and decreased steeply with depth in the main basin of the reservoir (Figs.
262 2C, 3). Average O_2 concentration in the downstream river was higher than in the hypoxic

hypolimnion of the reservoir, demonstrating that hypolimnetic waters get quickly oxygenated once leaving the turbines, despite not being as oxygenated as the upstream river or the surface mixed layer of the reservoir (Fig. 2C).

3.2. Relative abundance of MOB in DNA and RNA samples and abundance of MOB cells

The relative abundance of total MOB DNA and RNA sequences in the bacterial communities varied widely across samples with an average of 3.7% ± 5.8 (±SD) and 10.4% ± 15.2 of total 16S rRNA sequences in DNA and RNA, respectively. MOB sequences in upstream waters comprised on average 2.5% of the total sequences in DNA and 4.3% of the total sequences in RNA (Figs. 2D, E). In the reservoir, the relative abundance of MOB sequences was negligible in the mixed layer but increased in the oxic hypolimnion and reached extremely high values in the hypoxic hypolimnion (up to 27.6% for DNA and 61.2% for RNA), in line with the reduction in CH_4 concentration and enrichment in $\delta^{13}CH_4$ values in this layer observed in the profiles. The downstream river also showed high MOB relative abundances, with MOB sequences accounting for 8.5% ± 3.2 of total 16S rRNA sequences in DNA and 25.4% ± 7 in RNA across campaigns (Figs. 2D, E). Across all samples, the relative abundance of MOB sequences based on RNA was on average three times higher than that based on DNA.

The total MOB cell counts assessed by CARD-FISH showed a similar spatial pattern to that of the DNA and RNA data. The highest MOB cell abundance was measured in the hypoxic hypolimnion in 2017 (median: 6 x 10^4 cells mL^{-1}) followed by the downstream river (median: 4.1 x 10^4 cells mL^{-1}) and upstream sampling sites (median: 3.7 x 10^4 cells mL^{-1}) (Fig. 2F). In terms of

relative abundances, the highest contribution of MOB cells to total bacterial cells was also detected in the hypoxic hypolimnion of the reservoir, where MOB-hybridized cells made up to 19.2 % of total prokaryotic counts (details not shown). The abundance of total MOB cells was weakly but positively correlated to $\delta^{13}CH_4$ ($p=0.01$, $R^2=0.16$; Fig. S1A) across the sampled zones in the river-reservoir system, indicating that MOB cell number is related to methanotrophic activity. The relative abundance of MOB 16S rRNA sequences in DNA and RNA, however, were not significantly related to $\delta^{13}CH_4$ ($p>0.05$; Fig. S1B, C).

3.3. MOB diversity

A total of 271 amplicon sequence variants (ASVs) belonging to 21 MOB genera were detected across the whole dataset. Of these, 237 ASVs (15 genera) belonged to the Order Methylococcales (Gammaproteobacteria), 9 ASVs (2 genera) belonged to the Family Methylocystaceae (Alphaproteobacteria), 1 ASV (1 genus) belonged to the Family Beijerinckiaceae (Alphaproteobacteria), and 24 ASVs (3 genera) belonged to the putative methanotrophs within the Order Methylomirabilales (candidate phyla NC10) (Fig. S2). No Verrucomicrobia methanotrophs were detected. 48 ASVs within the Family Methylomonaceae (Order Methylococcales, Gammaproteobacteria) and 17 ASVs within the Family Methylococcaceae (Order Methylococcales, Gammaproteobacteria) could not be assigned at the genus level. The unclassified Methylomonaceae ASVs are related to *Methylomonas rubra* (NR_114588.1; 91% identity on average), while the unclassified Methylococcaceae ASVs are related to *Methylococcus capsulatus* (NR_042183.1) and *Methylocaldum marinum* (NR_126189.1; 90% identity on average; NCBI Nucleotide BLAST tool). Within the Gamma-MOB,

24 ASVs belonged to the filamentous methanotrophic bacteria of the genus *Crenothrix* (Stoecker et al., 2006).

MOB sequences were detected in every sampled zone of the river-reservoir system, but in only 6 out of 16 samples from the reservoir surface mixed layer (DNA and RNA; Fig. S2). On average, 69.7% of the total MOB DNA sequences belonged to Gammaproteobacteria, 28.3% to Alphaproteobacteria, and 2% to the NC10 candidate phyla across the samples in which MOB were detected (Fig. S3). In terms of RNA, the pattern was similar, with Gammaproteobacteria comprising on average 69.9% of the total MOB RNA sequences, followed by Alphaproteobacteria (29.4%) and the NC10 candidate phyla (0.7%, Fig. S3).

3.4. Dynamics of major MOB groups along the river-reservoir system

The MOB community composition changed along the river-reservoir system at the major groups level in terms of both cells and sequences abundance. While average Alpha- and Gamma-MOB cell counts were not significantly different in upstream and reservoir waters ($p>0.05$; Welch's unequal variances t-test on the log data), Alpha-MOB cells were more abundant than Gamma-MOB cells in the downstream river after the dam ($p=0.008$, Welch's unequal variances t-test on the log data; Fig. 4A). Also, average Alpha-MOB cell abundance increased from upstream to downstream waters. Both MOB groups showed maximum local cell abundances in the hypoxic hypolimnion of the reservoir, reaching 6.1×10^4 and 9.5×10^4 cells mL^{-1} for Alpha- and Gamma-MOB, respectively (Fig. 4A).

Both Alpha- and Gamma-MOB 16S rRNA sequences were detected in every site of the river-reservoir system. However, Gamma-MOB sequences clearly dominated the upstream waters while the relative abundance of Alpha-MOB sequences increased in the reservoir, where both groups showed similar contribution to total MOB sequences (Fig. 4B). NC10 sequences were detected at low abundances in upstream waters but reached up to 32% of the total MOB DNA sequences in one specific site at 32 m deep (Fig. 4B). In the downstream river, MOB sequences belonged to Alpha- and Gamma-MOB, while NC10 sequences were negligible. In general, the dynamics of these groups were similar in DNA and RNA and between sampling campaigns (Fig. 4B).

The relative abundance of 16S rRNA sequences belonging to total, Alpha-, and Gamma-MOB were significantly correlated ($p<0.05$) to the absolute cell counts determined by CARD-FISH (Fig. S4). However, sequencing overestimated the abundance of Gamma-MOB cells on average 1.88 times, while it underestimated the Alpha-MOB cell abundance in 20% on average (Fig. S4).

3.5. Environmental drivers and connectivity of MOB communities

We performed Canonical Analysis of Principal Coordinates (CAP) analyses based on the DNA and RNA profiles of MOB communities to investigate the similarity between MOB communities from different locations within the river-reservoir system and their links to environmental drivers (Fig. 5). Temperature, pH, CH_4 and O_2 concentrations significantly predicted patterns in MOB community structure across the studied system ($p=0.001$), but only explained a limited portion of the variation (Fig. 5), suggesting that unmeasured factors might

also contribute to the reported patterns in MOB assemblages. Dissolved organic carbon (DOC) concentration was not a significant ($p>0.05$) factor despite the potential role of DOC in MOB activity and community structure (Reis et al., 2020; Thottathil et al., 2018). This lack of effect of DOC is likely due to the absence of a gradient in DOC concentration, which is constantly very low (mean 0.9 mg L^{-1} ± 0.2 SD) in the reservoir (Soued and Prairie, 2020). Overall, patterns were similar between DNA, RNA, and both sampling campaigns, and MOB communities from the same location often grouped together (Fig. 5A, B). MOB communities from the upstream and reservoir mixed layer correlated positively with temperature, O_2, and pH while the oxic hypolimnion communities were spread across the CAP space. Downstream communities and hypoxic hypolimnetic MOB communities, however, grouped closely together reflecting the position of the water intake for the turbines and correlated with CH_4 concentration. In addition, the number of MOB ASVs increased along the continuum, reaching the highest taxonomic richness in the MOB communities in the downstream river (Fig. 5A, B).

To check whether the observed changes in MOB communities along the river-reservoir continuum resulted from taxa replacement as opposed to changes in the abundances of existing taxa, we categorized each ASV depending on the location where they were first detected (as in Ruiz-González et al. 2015a). We observed that in most locations, a large fraction of the ASVs was already detected in the upstream sites, making up more than 50% of the MOB DNA sequences even in the farthest downstream site sampled (Fig. 5C). Besides these 'upstream' ASVs, downstream MOB communities contained a large fraction of ASVs deriving from both the oxic and the hypoxic hypolimnion, but only a negligible proportion of sequences belonging to ASVs first detected in the surface mixed layer of the reservoir (Fig. 5C). 'Mixed

layer' unique ASVs were detected in 2018 and belonged to Gamma-MOB (Ca. *Methylospira*, *Methylocaldum*, and an unclassified genus; details not shown). Few MOB ASVs unique to the downstream sites (*i.e.* not present in the reservoir or in upstream waters) were detected (7 in 2017 and 27 in 2018), but they accounted for a very small fraction of the total MOB sequences (Fig. 5C). In both years, these 'downstream' unique MOB ASVs belonged to Gamma-MOB and NC10 (*Methylomonas*, *Methylosoma*, candidatus *Methylospira, Methylomagnum*, and *Methyloparacoccus* from Gamma-MOB*,* and unclassified genera from both groups; details not shown).

3.6. CH_4 oxidation and MOB cells dynamics in downstream waters

Based on the DNA and RNA compositional data it seemed that downstream MOB communities were merely hypolimnetic communities transported through the turbine tunnels (Fig. 5A, B). However, the CARD-FISH count data indicated a shift in the cell abundance of the two proteobacterial MOB groups from the hypolimnion to the downstream river, leading to significantly higher abundances of Alpha- than Gamma-MOB in the outflowing river waters (Fig. 4A). We thus investigated whether this shift was correlated to CH_4 oxidation in the downstream river by following the CH_4 concentration and stable isotopic signature, O_2 concentration, and Alpha- and Gamma-MOB cell abundance from the water intake for the turbines in the hypolimnion of the reservoir until 2.7 Km downstream from the dam (Fig. 6). The reduction in CH_4 concentration and simultaneous increase in stable isotopic signature of the remaining CH_4 indicated microbial CH_4 oxidation within downstream waters in both years (Fig. 6A, B). We found that the fraction of CH_4 oxidized (*F*ox) within the river segment was higher in 2017 than

393 in 2018 (Fig. 6C), but that the absolute amount of CH_4 oxidized was higher in 2018 than in 2017
394 (Fig. 6D) because the CH_4 concentration at the turbine water intake was much higher in 2018
395 than in 2017 (82 and 52 µM, respectively; Fig. 6A). O_2 concentration in the water was higher in
396 2017 than in 2018 both before and after its passage through the turbines (Fig. 6E). The cell
397 abundances of both MOB groups decreased between the turbines' intake in the reservoir and
398 the power station (0 Km) in 2017 (Fig. 6F), which could be caused by death of cells but also by
399 dilution since the turbines draw water from a wide range of depths. However, once in the
400 downstream river, Alpha-MOB cell abundance quickly increased along the river segment in
401 2017 and 2018 (Fig. 6F). In both years, Alpha-MOB clearly dominated over Gamma-MOB at 2.7
402 Km, where highest *F*ox and absolute amount of CH_4 oxidized were also observed.
403

404 **4. DISCUSSION**

405 Despite the central role of MOB in regulating CH_4 emissions from hydropower
406 reservoirs, very few studies have investigated MOB communities in these systems (Dumestre et
407 al., 1999; Itoh et al., 2015). In particular, although the importance of CH_4 oxidation has also
408 been recognized in downstream waters, no study has explored how MOB communities respond
409 to drastic environmental changes from the hypoliminia of reservoirs to rapidly re-oxygenated
410 turbine outflowing waters. This is of special interest in lower latitudes, given that tropical
411 hydropower reservoirs are often strongly stratified, reducing the importance of CH_4 diffusive
412 fluxes through the reservoir surface and making downstream CH_4 emissions particularly
413 important (Guérin et al., 2006; Soued and Prairie, 2020). Here we show that in the narrow band
414 of environmental conditions that are optimal for CH_4 oxidation to occur, MOB abundance and

potential activity can reach very high levels (up to 27% and 61% of the total bacterial DNA and RNA sequences, respectively). This spatial confinement of abundant and highly active MOB communities in the hypoxic zone of the hypolimnion of Batang Ai, which creates a CH_4 concentration minimum in the oxic hypolimnion, imposes a biogeochemical disconnection between the hypolimnetic CH_4 and the reservoir surface CH_4 emissions. We also show that MOB taxa in Batang Ai are to a large extent sourced from upstream waters, but that environmental gradients generated by the dam allow the local establishment of different and specific MOB communities in the different zones of the hydropower complex. In addition, by microscopically quantifying MOB cells, we show that fast cell growth of mostly Alpha-MOB taxa in downstream waters happens simultaneously with CH_4 oxidation in well-oxygenated downstream waters.

4.1. High total MOB DNA and RNA sequences in Batang Ai reservoir

We found high relative abundances of MOB 16S rRNA sequences in DNA and RNA in the hypoxic hypolimnion of the tropical reservoir Batang Ai (up to 27% and 61% of total bacterial DNA and RNA sequences, respectively), and these belonged to methanotrophic taxa in the Gammaproteobacteria and Alphaproteobacteria classes. NC10 putative methanotrophs were only abundant in our deepest sample in anoxic waters within the reservoir (32 m) where they accounted for almost one third of the total MOB DNA sequences. Similarly, NC10 putative methanotrophs have been found to constitute a significant portion of the active methanotrophic community in anoxic zones of lakes and reservoirs (Deutzmann et al., 2014; Kojima et al., 2014). The peak in total MOB abundances in hypoxic waters observed in our study

437 is in line with previous studies reporting highest MOB abundances at oxic-anoxic interfaces in
438 other lakes and reservoirs (Dumestre et al., 1999; Kojima et al., 2014; Mayr et al., 2019; Reis et
439 al., 2020). Comparatively high relative abundances of MOB sequences have been detected in
440 permafrost thaw ponds (maximum 27% of the 16S rRNA sequences; Crevecoeur et al. 2015),
441 temperate lakes (11-26% of total 16S rRNA gene sequences; Mayr et al. 2019), a subtropical
442 reservoir (maximum ~30% of total 16S rRNA gene sequences; Kojima et al. 2015), and a tropical
443 hydropower reservoir (up to 24% of DGGE-obtained sequences; Dumestre et al. 2001).
444 Regarding MOB RNA sequences, our values (up to 61%) represent the highest reported values
445 of MOB abundance in freshwaters to our knowledge and suggests that CH_4 defines a clear
446 microbial niche in the hypolimnion of the Batang Ai reservoir with MOB making a large fraction
447 of the protein synthesizing bacterial community in this layer. Indeed, the high MOB abundance
448 in the hypoxic hypolimnion, together with the decrease in CH_4 concentration and enrichment of
449 $\delta^{13}CH_4$ (Fig. 2A, 3), indicates intense methanotrophic activity and that most of the upward flux
450 of CH_4 is oxidized by MOB in the hypoxic zone of the reservoir, as observed in other permanent
451 stratified lakes and reservoirs (*e.g.* Borges et al. 2011; Itoh et al. 2015).

452 In general, the patterns observed in the DNA and RNA MOB sequences were quite
453 similar indicating that the present MOB taxa are potentially active across the sampled zones in
454 Batang Ai. An exception to this tight coupling between DNA and RNA was observed in the
455 reservoir mixed layer, where DNA and RNA patterns were particularly variable (Fig. 3B, 4A)
456 probably due to the very low relative abundances of total MOB 16S rRNA sequences in this
457 layer (<0.1% of total 16S rRNA gene sequences) (Fig. 2D, E).

458

4.2. Hydrologic connectivity of MOB communities along the river-reservoir system

Downstream bacterial communities showed high proportions of MOB sequences and cells, and MOB communities from downstream sites clustered very closely together with those from the hypoxic hypolimnion, differing largely from upstream and mixed layer assemblages (Fig. 5A, B). By tracing the origin of ASVs along the studied system, we observed that a large fraction of the downstream MOB communities comprised taxa first detected in both oxic and hypoxic hypolimnetic sites. In 2018, the fraction of MOB ASVs from the hypoxic hypolimnion in the downstream river was higher than in 2017, while MOB ASVs first detected in the oxic hypolimnion were more abundant in the downstream river in 2017 than in 2018. This difference in the source of downstream MOB taxa is likely related to the variation in the reservoir's water level, which affects the water withdrawal depth. Only a few unique downstream MOB ASVs were detected, showing that although downstream conditions allow for the establishment of new MOB taxa, downstream MOB communities are almost entirely dominated by taxa dispersed from upstream reservoir sites. Moreover, although all sampled locations harbored a large fraction of taxa originating in the rivers flowing into the reservoir, most MOB ASVs specific to the mixed layer did not reach downstream waters. This reflects the discontinuity in surface water flow caused by the stratification within the reservoir and the position of the turbines' water intake. These unique ASVs from the mixed layer were only detected in 2018, while in 2017 all the MOB ASVs detected in the mixed layer were also detected in the upstream sites. Interestingly, upstream riverine waters were much warmer in 2017 (30.6 °C) than in 2018 (26.1 °C) at 1 m depth, suggesting that inflowing upstream waters mixed well with the reservoir's mixed layer (average temperature 31 °C) in 2017 but likely sank

481 below it while entering the reservoir in 2018. This supports the larger connectivity between the
482 upstream and the mixed layer communities in 2017 than in 2018 shown by the analysis of the
483 origin of MOB ASVs.

484 The importance of hydrologic connectivity in shaping the structure of freshwater
485 bacterioplankton has been shown for whole communities (Niño-García et al., 2016; Ruiz-
486 González et al., 2015a, 2013) and specifically for MOB assemblages across boreal lakes and
487 rivers (Crevecoeur et al., 2019). Here we show that although reservoir MOB communities are
488 sourced to a large extent from upstream rivers, the specific environmental conditions and the
489 permanent stratification generated within the reservoir cause the establishment of MOB
490 communities and taxa specific to each reservoir zone. By disconnecting surface waters but
491 connecting the hypolimnion of the reservoir to the river downstream, the damming of the
492 Batang Ai river creates a break in the connectivity between upstream and downstream MOB
493 assemblages and a drastic change in oxygen conditions between the hypolimnion of the
494 reservoir and the downstream river. Yet, rapid shifts in the MOB community in the first few
495 kilometers downstream of the dam enabled continued CH_4 oxidation in the river downstream.

496

497 *4.3. Differential growth of MOB groups in the downstream river and links to CH_4*
498 *oxidation*

499 Based solely on our sequencing results, CH_4 oxidation in the downstream river below
500 the Batang Ai dam is apparently the result of the residual activity of MOB hypolimnetic
501 communities since they are similar in composition (Fig. 5A, B), with very few new MOB ASVs
502 detected in the downstream reach (Fig. 5C). However, the enumeration of MOB cells by CARD-

FISH revealed a rapid growth of Alpha-MOB cells within the downstream river if compared to Gamma-MOB cells. These Alpha-MOB cells belonged to taxa that were already present in the hypolimnion of the reservoir, given that none of the unique 'downstream' ASVs belonged to Alpha-MOB, but were favored under the downstream environmental conditions such as both high CH_4 and higher O_2 concentrations (Reis et al., 2020). A higher role of Alpha-MOB over Gamma-MOB in downstream waters is supported by a strong correlation between the amount of CH_4 oxidized in each segment of the river and Alpha-MOB cells (R^2=0.98, p=0.005) and the lack of correlation with Gamma-MOB cells (R^2=0.04, p=0.78) (Fig S5), although only four data points are available. Microscopic visualization also revealed that Alpha-MOB cells occurred often in pairs, potentially indicating that cells were actively dividing in this segment of the downstream river (Fig. S6).

The measured increase in MOB cell numbers represents an extremely rapid response of methanotrophic taxa to changes in the environment rather than just a passive dispersal of hypolimnetic communities. It also represents an extremely fast cell growth rate given the short time interval between the power station (0 km) and 2.7 Km further downstream (approx. 1 h, flow rate of ~ 1 m s^{-1}, unpubl. data). Under the high CH_4 and oxygenated conditions in the downstream river, Alpha-MOB cells showed a surprisingly short average doubling time of 1.7 h, while Gamma-MOB showed a longer but also short average doubling time of 2.3 h. These are in the low range of estimated prokaryotic doubling times in nature – which can vary from minutes to days (Gibson et al., 2018) – and of methanotrophic bacteria doubling times in pure cultures (Baani and Liesack, 2008; Puri et al., 2015; Sundstrom and Criddle, 2015), suggesting that the

524 downstream river meets ideal growth conditions to some MOB taxa, particularly within the
525 Alpha-MOB group.

526 To verify whether such fast MOB growth observed by the CARD-FISH enumeration was
527 metabolically possible, we estimated the increase in MOB cell abundance in the downstream
528 segment based on the amount of CH_4 oxidized, the average MOB cell volume (calculated from
529 the area of the DAPI subset of FISH positive cells in this dataset), an assumed MOB growth
530 efficiency of 10%, and a bacterial cell carbon content of 63 fgC μm^{-3} (Fagerbakke et al., 1996)
531 (see details in Suppl. Info.). We found that the total MOB cell increase measured by CARD-FISH
532 was lower than the calculated MOB cell increase (on average 33% lower). We performed
533 sensitivity tests by decreasing the assumed MOB growth efficiency to 5% or increasing the cell
534 carbon content to 126 fgC μm^{-3}, and in both scenarios the measured MOB cell increase by
535 CARD-FISH could be fully accounted by the amount of CH_4 oxidized within the reach.
536 Interestingly, the total amount of carbon fixed by microbial CH_4 oxidation in the studied river
537 segment varied between 210 and 306 mgC m^{-2} d^{-1} between the years, which is in the upper
538 range of carbon fixation by primary production in tropical rivers generally reported (10-200
539 mgC m^{-2} d^{-1}; Davies et al. 2008). This suggests that CH_4 is likely an important basal carbon
540 source to the food web of the oligotrophic (chlorophyll-a: 1.7 ± 0.8 µg L^{-1}) river downstream of
541 the Batang Ai dam.

542

543 *4.4. The importance of combining microscopy and sequencing data for the study of*
544 *MOB communities*

In the present study, the sequencing data allowed tracking changes in MOB communities and individual ASVs along the river-reservoir system, enabling the observation of spatial changes in the taxonomic composition and connectivity of the studied communities. However, a link between community shift and CH_4 oxidation in the downstream river could only be determined due to the microscopic cell enumeration, since the sequencing data did not allow the detection of fast quantitative differences between the source hypolimnetic communities and downstream MOB communities, which looked similar based on the sequencing data. Therefore, our study demonstrates the importance of combining high-resolution sequencing data with microscopic quantitative data for attaining a more complete understanding of MOB dynamics and activity in the environment.

5. CONCLUSION

Our study of the MOB dynamics in a tropical reservoir contributes to better understanding the mechanisms by which these bacteria play a central role in modulating the carbon footprint of aquatic ecosystems and, in particular, of hydropower complexes. By combining biogeochemical data, DNA and RNA sequencing, and cell enumeration, we found that CH_4 dynamics are accompanied by shifts in the total abundance and structure of MOB communities along the Batang Ai river-reservoir system. In the main basin of the reservoir, where diffusive CH_4 emissions are only moderate (Soued and Prairie, 2020), MOB sequences, cells, and activity peak in the hypoxic hypolimnion (up to 61% of 16S rRNA sequences and enriched $\delta^{13}CH_4$), disconnecting the hypolimnetic CH_4 from surface CH_4 emissions to the atmosphere. While most of the MOB taxa present across the system is dispersed from

upstream sites, downstream MOB communities resemble reservoir's hypolimnetic communities but differ largely from upstream and mixed layer communities due to the position of the water intake for the turbines. When CH_4-rich hypolimnetic water is released to the downstream river, the re-oxygenation seems to promote the activity and fast growth of particularly Alpha-MOB taxa that are already present in the hypolimnion of the reservoir. Therefore, although downstream emissions constitute a major pathway of CH_4 emissions in Batang Ai (Soued and Prairie 2020) and in other hydropower complexes, rapid shifts in the MOB community enable continued microbial CH_4 oxidation in the downstream river, thereby contributing to lowering the carbon footprint of these systems.

Declaration of competing interests

The authors declare no competing interests.

Acknowledgements

The authors thank Karen Lee Suan Ping, Jenny Choo Cheng Yi, Amar Ma'aruf Bin Ismawi and Gerald Tawie Anak Thomas for their logistic support and great help in the field. We are also grateful to Jenny Choo Cheng Yi for her support in the molecular laboratory. This study was supported by Natural Sciences and Engineering Research Council of Canada Discovery grants and Sarawak Energy Berhad and is a contribution to UNESCO Chair in Global Environmental Change. We also acknowledge financial support from the Groupe de recherche interuniversitaire en limnologie (GRIL), a strategic cluster of the Fonds de recherche du Québec

588 - Nature et technologies (FRQNT). PCJR was supported by a merit doctoral scholarship from the
589 Fonds de recherche du Québec - Nature et technologies (FRQNT).

590

591 **REFERENCES**

592 Abril, G., Guérin, F., Richard, S., Delmas, R., Galy-Lacaux, C., Gosse, P., Tremblay, A., Varfalvy, L.,
593 Dos Santos, M.A., Matvienko, B., 2005. Carbon dioxide and methane emissions and the
594 carbon budget of a 10-year old tropical reservoir (Petit Saut, French Guiana). Global
595 Biogeochem. Cycles 19, 1–16. https://doi.org/10.1029/2005GB002457

596 Anderson, M.J., Willis, T.J., 2003. Canonical analysis of principal coordinates: a useful method of
597 constrained ordination for ecology. Ecology 84, 511–525.

598 Baani, M., Liesack, W., 2008. Two isozymes of particulate methane monooxygenase with
599 different methane oxidation kinetics are found in Methylocystis sp. strain SC2. Proc. Natl.
600 Acad. Sci. U. S. A. 105, 10203–8. https://doi.org/10.1073/pnas.0702643105

601 Barros, N., Cole, J.J., Tranvik, L.J., Prairie, Y.T., Bastviken, D., Huszar, V.L.M., del Giorgio, P.,
602 Roland, F., 2011. Carbon emission from hydroelectric reservoirs linked to reservoir age and
603 latitude. Nat. Geosci. 4, 593–596. https://doi.org/10.1038/ngeo1211

604 Blazewicz, S.J., Barnard, R.L., Daly, R.A., Firestone, M.K., 2013. Evaluating rRNA as an indicator
605 of microbial activity in environmental communities: limitations and uses. ISME J. 7, 2061–
606 2068. https://doi.org/10.1038/ismej.2013.102

607 Borrel, G., Jézéquel, D., Biderre-Petit, C., Morel-Desrosiers, N., Morel, J.P., Peyret, P., Fonty, G.,
608 Lehours, A.C., 2011. Production and consumption of methane in freshwater lake

609 ecosystems. Res. Microbiol. 162, 833–847. https://doi.org/10.1016/j.resmic.2011.06.004

610 Callahan, B.J., McMurdie, P.J., Rosen, M.J., Han, A.W., Johnson, A.J.A., Holmes, S.P., 2016.
611 DADA2: High-resolution sample inference from Illumina amplicon data. Nat. Methods 13,
612 581–583. https://doi.org/10.1038/nmeth.3869

613 Coleman, D.D., Risatti, J.B., Schoell, M., 1981. Fractionation of carbon and hydrogen isotopes by
614 methane-oxidizing bacteria. Geochim. Cosmochim. Acta 45, 1033–1037.
615 https://doi.org/10.1016/0016-7037(81)90129-0

616 Conrad, R., 2007. Microbial Ecology of Methanogens and Methanotrophs. Adv. Agron. 96, 1–63.
617 https://doi.org/10.1016/S0065-2113(07)96005-8

618 Crevecoeur, S., Ruiz-González, C., Prairie, Y.T., del Giorgio, P.A., 2019. Large scale biogeography
619 and environmental regulation of methanotrophic bacteria across boreal inland waters. in
620 press. Mol. Ecol. https://doi.org/10.1111/mec.15223

621 Davies, P.M., Bunn, S.E., Hamilton, S.K., 2008. Primary production in tropical streams and rivers,
622 in: Tropical Stream Ecology. pp. 23–42. https://doi.org/10.1016/B978-012088449-0.50004-
623 2

624 Deemer, B.R., Harrison, J.A., Li, S., Beaulieu, J.J., DelSontro, T., Barros, N.O., Bezerra-Neto, J.F.,
625 Powers, S.M., Dos Santos, M.A., Vonk, j A., 2016. Greenhouse Gas Emissions from
626 Reservoir Water Surfaces: A New Global Synthesis. Bioscience XX.
627 https://doi.org/10.1093/biosci/biw117

628 Deutzmann, J.S., Stief, P., Brandes, J., Schink, B., 2014. Anaerobic methane oxidation coupled to

denitrification is the dominant methane sink in a deep lake. Proc. Natl. Acad. Sci. 111, 18273–18278. https://doi.org/10.1073/pnas.1411617111

Dumestre, J., Guézennec, J., Galy-Lacaux, C., Delmas, R., Richard, S., Labroue, L., 1999. Influence of light intensity on methanotrophic bacterial activity in Petit Saut reservoir, French Guiana. Appl. Environ. Microbiol. 65, 534–539.

Dumestre, J.F., Vaquer, A., Gosse, P., Richard, S., Labroue, L., 1999. Bacterial ecology of a young equatorial hydroelectric reservoir (Petit Saut, French Guiana): Evidence of reduced compound exhaustion and bacterial community adaptation. Hydrobiologia 400, 75–83. https://doi.org/10.1023/A:1003707129170

Dunfield, P.F., Yuryev, A., Senin, P., Smirnova, A. V, Stott, M.B., Hou, S., Ly, B., Saw, J.H., Zhou, Z., Ren, Y., Wang, J., Mountain, B.W., Crowe, M. a, Weatherby, T.M., Bodelier, P.L.E., Liesack, W., Feng, L., Wang, L., Alam, M., 2007. Methane oxidation by an extremely acidophilic bacterium of the phylum Verrucomicrobia. Nature 450, 879–882. https://doi.org/10.1038/nature06411

Eller, G., Stubner, S., Frenzel, P., 2001. Group-specific 16S rRNA targeted probes for the detection of type I and type II methanotrophs by fluorescence in situ hybridisation. FEMS Microbiol. Lett. 198, 91–97.

Ettwig, K.F., Butler, M.K., Le Paslier, D., Pelletier, E., Mangenot, S., Kuypers, M.M.M., Schreiber, F., Dutilh, B.E., Zedelius, J., de Beer, D., Gloerich, J., Wessels, H.J.C.T., van Alen, T., Luesken, F., Wu, M.L., van de Pas-Schoonen, K.T., Op den Camp, H.J.M., Janssen-Megens, E.M., Francoijs, K.-J., Stunnenberg, H., Weissenbach, J., Jetten, M.S.M., Strous, M., 2010. Nitrite-

650 driven anaerobic methane oxidation by oxygenic bacteria. Nature 464, 543–548.
651 https://doi.org/10.1038/nature08883

652 Fagerbakke, K.M., Heldal, M., Norland, S., 1996. Content of carbon, nitrogen, oxygen, sulfur and
653 phosphorus in native aquatic and cultured bacteria. Aquat. Microb. Ecol. 10, 15–27.
654 https://doi.org/10.3354/ame010015

655 Gibson, B., Wilson, D.J., Feil, E., Eyre-walker, A., Eyre-walker, A., 2018. The distribution of
656 bacterial doubling times in the wild.

657 Guérin, F., Abril, G., 2007. Significance of pelagic aerobic methane oxidation in the methane and
658 carbon budget of a tropical reservoir. J. Geophys. Res. 112, 1–14.
659 https://doi.org/10.1029/2006JG000393

660 Guérin, F., Abril, G., Richard, S., Burban, B., Reynouard, C., Seyler, P., Delmas, R., 2006. Methane
661 and carbon dioxide emissions from tropical reservoirs: Significance of downstream rivers.
662 Geophys. Res. Lett. 33, 1–6. https://doi.org/10.1029/2006GL027929

663 Hanson, R.S., Hanson, T.E., 1996. Methanotrophic bacteria. Microbiol. Rev. 60, 439–471.

664 Ho, A., Kerckhof, F.-M., Luke, C., Reim, A., Krause, S., Boon, N., Bodelier, P.L.E., 2013.
665 Conceptualizing functional traits and ecological characteristics of methane-oxidizing
666 bacteria as life strategies. Environ. Microbiol. Rep. 5, 335–345.
667 https://doi.org/10.1111/j.1758-2229.2012.00370.x

668 Itoh, M., Kobayashi, Y., Chen, T.Y., Tokida, T., Fukui, M., Kojima, H., Miki, T., Tayasu, I., Shiah,
669 F.K., Okuda, N., 2015. Effect of interannual variation in winter vertical mixing on CH4

dynamics in a subtropical reservoir. J. Geophys. Res. Biogeosciences 120, 1246–1261. https://doi.org/10.1002/2015JG002972

Kalyuzhnaya, M.G., Gomez, O.A., Murrell, J.C., 2019. The Methane-Oxidizing Bacteria (Methanotrophs), in: Taxonomy, Genomics and Ecophysiology of Hydrocarbon-Degrading Microbes. pp. 1–34. https://doi.org/10.1007/978-3-319-60053-6_10-1

Kemenes, A., Forsberg, B.R., Melack, J.M., 2007. Methane release below a tropical hydroelectric dam. Geophys. Res. Lett. 34, 1–5. https://doi.org/10.1029/2007GL029479

Knief, C., 2015. Diversity and habitat preferences of cultivated and uncultivated aerobic methanotrophic bacteria evaluated based on pmoA as molecular marker. Front. Microbiol. 6, 1346. https://doi.org/10.3389/fmicb.2015.01346

Kojima, H., Tokizawa, R., Kogure, K., Kobayashi, Y., Itoh, M., Shiah, F., Okuda, N., Fukui, M., 2014. Community structure of planktonic methane-oxidizing bacteria in a subtropical reservoir characterized by dominance of phylotype closely related to nitrite reducer. Sci. Rep. 4, 1–7. https://doi.org/10.1038/srep05728

Mayr, M.J., Zimmermann, M., Guggenheim, C., Brand, A., Bürgmann, H., 2019. Niche partitioning of methane-oxidizing bacteria in the oxygen-methane counter gradient of stratified lakes. Isme in review. https://doi.org/10.1038/s41396-019-0515-8

Mcmurdie, P.J., Holmes, S., 2013. phyloseq : An R Package for Reproducible Interactive Analysis and Graphics of Microbiome Census Data 8. https://doi.org/10.1371/journal.pone.0061217

690 Niño-García, J.P., Ruiz-González, C., Del Giorgio, P.A., 2016. Interactions between hydrology and
691 water chemistry shape bacterioplankton biogeography across boreal freshwater networks.
692 ISME J. 10, 1755–1766. https://doi.org/10.1038/ismej.2015.226

693 Oswald, K., Milucka, J., Brand, A., Hach, P., Littmann, S., Wehrli, B., Kuypers, M.M.M., Schubert,
694 C.J., 2016. Aerobic gammaproteobacterial methanotrophs mitigate methane emissions
695 from oxic and anoxic lake waters. Limnol. Oceanogr. 61, S101–S118.
696 https://doi.org/10.1002/lno.10312

697 Prairie, Y.T., Alm, J., Beaulieu, J., Barros, N., Battin, T., Cole, J., Del Giorgio, P., DelSontro, T.,
698 Guérin, F., Harby, A., Harrison, J., Mercier-Blais, S., Serça, D., Sobek, S., Vachon, D., 2017.
699 Greenhouse Gas Emissions from Freshwater Reservoirs: What Does the Atmosphere See?
700 Ecosystems 1–14. https://doi.org/10.1007/s10021-017-0198-9

701 Puri, A.W., Owen, S., Chu, F., Chavkin, T., Beck, D.A.C., Kalyuzhnaya, M.G., Lidstrom, M.E., 2015.
702 Genetic tools for the industrially promising methanotroph Methylomicrobium buryatense.
703 Appl. Environ. Microbiol. 81, 1775–1781. https://doi.org/10.1128/AEM.03795-14

704 Reis, P.C.J., Thottathil, S.D., Ruiz-González, C., Prairie, Y.T., 2020. Niche separation within
705 aerobic methanotrophic bacteria across lakes and its link to methane oxidation rates.
706 Environ. Microbiol. 22, 738–751. https://doi.org/10.1111/1462-2920.14877

707 Rissanen, A.J., Saarenheimo, J., Tiirola, M., Peura, S., Aalto, S.L., Karvinen, A., Nykänen, H., 2018.
708 Gammaproteobacterial methanotrophs dominate methanotrophy in aerobic and
709 anaerobic layers of boreal lake waters. Aquat. Microb. Ecol. 81, 257–276.
710 https://doi.org/10.3354/ame01874

RStudio, T., 2018. RStudio: Integrated Development for R.

Rudd, J.W.M., Hamilton, R.D., Campbell, N.E.R., 1974. Measurement of microbial oxidation of methane in lake water 19, 519–524.

Ruiz-González, C., Niño-García, J.P., del Giorgio, P.A., 2015a. Terrestrial origin of bacterial communities in complex boreal freshwater networks. Ecol. Lett. 18, 1198–1206. https://doi.org/10.1111/ele.12499

Ruiz-González, C., Proia, L., Ferrera, I., Gasol, J.M., Sabater, S., 2013. Effects of large river dam regulation on bacterioplankton community structure. FEMS Microbiol. Ecol. 84, 316–331. https://doi.org/10.1111/1574-6941.12063

Ruiz-González, C., Salazar, G., Logares, R., Proia, L., Gasol, J.M., Sabater, S., 2015b. Weak coherence in abundance patterns between bacterial classes and their constituent OTUs along a regulated river. Front. Microbiol. 6, 1–13. https://doi.org/10.3389/fmicb.2015.01293

Soued, C., Prairie, Y.T., 2020. The carbon footprint of a Malaysian tropical reservoir : measured versus modeled estimates highlight the underestimated key role of downstream processes. Biogeosciences 17, 515–227. https://doi.org/10.5194/bg-2019-385

St. Louis, V.L., Kelly, C.A., Duchemin, É., Rudd, J.W.M., Rosenberg, D.M., 2000. Reservoir Surfaces as Sources of Greenhouse Gases to the Atmosphere: A Global Estimate. Bioscience 50, 766. https://doi.org/10.1641/0006-3568(2000)050[0766:rsasog]2.0.co;2

Steinle, L., Maltby, J., Treude, T., Kock, A., Bange, H.W., Engbersen, N., Zopfi, J., Lehmann, M.F.,

731 Niemann, H., 2017. Effects of low oxygen concentrations on aerobic methane oxidation in
732 seasonally hypoxic coastal waters. Biogeosciences 14, 1631–1645.
733 https://doi.org/10.5194/bg-14-1631-2017

734 Stoecker, K., Bendinger, B., Schöning, B., Nielsen, P.H., Nielsen, J.L., Baranyi, C., Toenshoff, E.R.,
735 Daims, H., Wagner, M., 2006. Cohn's Crenothrix is a filamentous methane oxidizer with an
736 unusual methane monooxygenase. Proc. Natl. Acad. Sci. U. S. A. 103, 2363–2367.
737 https://doi.org/10.1073/pnas.0506361103

738 Sundstrom, E.R., Criddle, C.S., 2015. Optimization of methanotrophic growth and production of
739 poly(3-hydroxybutyrate) in a high-throughput microbioreactor system. Appl. Environ.
740 Microbiol. 81, 4767–4773. https://doi.org/10.1128/AEM.00025-15

741 The R Core Team, 2019. R: A language and environment for statistical computing.

742 Thottathil, S.D., Reis, P.C.J., del Giorgio, P.A., Prairie, Y.T., 2018. The Extent and Regulation of
743 Summer Methane Oxidation in Northern Lakes. J. Geophys. Res. Biogeosciences 123,
744 3216–3230. https://doi.org/10.1029/2018JG004464

745 Thottathil, S.D., Reis, P.C.J., Prairie, Y.T., 2019. Methane oxidation kinetics in northern
746 freshwater lakes. Biogeochemistry 143, 105–116. https://doi.org/10.1007/s10533-019-
747 00552-x

748 Tremblay, A., Varfalvy, L., Roehm, C., Garneau, M., 2005. Synthesis, in: Tremblay, A., Varfalvy,
749 L., Roehm, C., Garneau, M. (Eds.), Greenhouse Gas Emissions - Fluxes and Processes:
750 Hydroelectric Reservoirs and Natural Environments. Springer, pp. 637–659.

751 Wang, Q., Garrity, G.M., Tiedje, J.M., Cole, J.R., 2007. Naïve Bayesian classifier for rapid
752 assignment of rRNA sequences into the new bacterial taxonomy. Appl. Environ. Microbiol.
753 73, 5261–5267. https://doi.org/10.1128/AEM.00062-07

754 Wickham, H., 2016. ggplot2: Elegant Graphics for Data Analysis.

755 Zeder, M., 2014. ACME tool3.

756 Zigah, P.K., Oswald, K., Brand, A., Dinkel, C., Wehrli, B., Schubert, C.J., 2015. Methane oxidation
757 pathways and associated methanotrophic communities in the water column of a tropical
758 lake. Limnol. Oceanogr. 60, 553–572. https://doi.org/10.1002/lno.10035

759
760
761
762
763
764
765
766
767
768
769
770
771

772 **FIGURES CAPTIONS**

773 Fig. 1. Map of Batang Ai hydropower reservoir (Borneo Island, Malaysia) showing sampling
774 locations of this study. Sites A, B, C, and I are located in the reservoir, with site I being the
775 closest to the water intake for the turbines. Sites E, F, G, and H are located upstream of the
776 reservoir. Site Dw-I is located at the power station right after the dam and Dw-II is located at
777 2.7 Km further downstream. One extra site at 0.6 Km downstream of the dam (not shown) was
778 sampled for CH_4 concentration and stable isotopic signature (see Fig. 6). Map created in ArcGIS
779 10.1.

780

781 Fig. 2. CH_4, O_2, and total methane-oxidizing bacteria (MOB) abundance along the Batang Ai
782 river-reservoir system. A) Dissolved CH_4 concentration (n = 36). B) CH_4 stable isotopic signature
783 (n = 32). C) Dissolved O_2 concentration (n = 34). D-E) Abundance of total MOB sequences
784 relative to the total bacterial community (%) in terms of DNA (n = 37) and RNA (n = 37)
785 sequences, respectively. F) Total MOB cell abundance determined by CARD-FISH (n = 20). MOB
786 cells were not determined in the mixed layer of the reservoir since the abundance of MOB 16S
787 rRNA sequences, when detected, was < 0.1% in this layer. Sampling locations are grouped as
788 shown in Fig. 1 with 'Res. Mix. Layer', 'Res. Oxic Hypo.', and 'Res. Hypoxic Hypo.' denoting the
789 surface mixed layer, the oxic layer of the hypolimnion (O_2 > 2 mg L^{-1}), and the hypoxic layer of
790 the hypolimnion (O_2 < 2 mg L^{-1}) within the reservoir. Boxplots represent median, first and third
791 quartiles (hinges), and 1.5 *x* interquartile range (whiskers). Diamonds denote means. Note log
792 scale in y axes of A and F.

793

Fig. 3. Vertical profiles of temperature, dissolved O_2 concentration, CH_4 concentration, and CH_4 stable isotopic signature measured in the main basin of the reservoir (site I) in 2018. Dashed red line: water temperature. Dashed blue line: dissolved O_2 concentration. Purple dots and line: CH_4 concentration. Green triangles and line: CH_4 stable isotopic signature. Asterisks show depths where samples for DNA and RNA were taken in this profile.

Fig. 4. Dynamics of major methane-oxidizing bacteria (MOB) groups from upstream to downstream waters in the Batang Ai river-reservoir system. A) Absolute abundances of Alpha-MOB and Gamma-MOB cells determined by CARD-FISH (n = 20). Boxplots represent median, first and third quartiles (hinges), and 1.5 *x* interquartile range (whiskers). Diamonds denote means and stars denote significant difference ($p<0.05$, Welch's unequal variances t-test) between average cell abundance of MOB groups within location. Note log scale in the y axis. Plotted data include both sampling campaigns. B) Relative abundance of DNA and RNA sequences belonging to major taxonomic MOB groups (sum of all MOB sequences in a sample = 1). Each bar represents a sample taken at a different campaign, site, and depth (n = 37). In the x axis, the letters indicate the site code as in Fig. 1, followed by two numbers indicating the sampling depth and the sampling campaign (2017 or 2018), respectively. Empty slots mean that MOB were not detected (Res. Mix. Layer) or that the sample was lost during rarefaction (n.a.; Res. Oxic Hypo. and Res. Hypoxic Hypo.). Res. Mix. Layer: reservoir's mixed layer; Res. Oxic Hypo.: reservoir's oxic hypolimnion; Res. Hypoxic Hypo.: reservoir's hypoxic hypolimnion.

Fig. 5. Dynamics of methane-oxidizing bacteria (MOB) communities along the river-reservoir system. A-B) Canonical Analysis of Principal Coordinates (CAP) based on Bray-Curtis distance of the DNA (p=0.001) and RNA (p=0.001) MOB community profiles, respectively. 32 samples that did not contain missing values were used in both DNA and RNA CAP analyses. C) Proportion of DNA and RNA MOB sequences associated to MOB ASVs categorized depending on the location of the river-reservoir system where they were first detected. Values are expressed as a fraction of the total MOB sequences for the different sampled sites and campaign. Res. Mix. Layer: reservoir mixed layer; Res. Oxic Hypo.: reservoir oxic hypolimnion; Res. Hypoxic Hypo.: reservoir hypoxic hypolimnion; Turb. Intake: closest available sample to the turbine water intake (2017: site A, depth 20 m; 2018: site I, depth 24 m); Downs0km: Downstream site at the power station; Downs2.7km: Downstream site at 2.7 km further downstream.

Fig. 6. CH_4 oxidation and MOB cell dynamics along the sampled sites from the turbines' water intake (located in the hypolimnion of the reservoir) until 2.7 Km downstream from the dam (the dam is indicated by the gray vertical bar). A) Dissolved CH_4 concentration. B) CH_4 stable isotopic signature. C) Cumulative fraction of CH_4 oxidized (*F*ox) calculated from the concentration and isotopic signature of CH_4 at each point using the turbine water intake as CH_4 source. D) Cumulative amount of CH_4 oxidized, calculated from *F*ox and CH_4 concentration. E) Dissolved O_2 concentration. F) Alpha- and Gamma-MOB cell abundances enumerated by CARD-FISH. The abundance of MOB cells entering the turbines was determined in the closest available sample to the turbine water intake (2017: site A, depth 20 m; 2018: site I, depth 24 m).

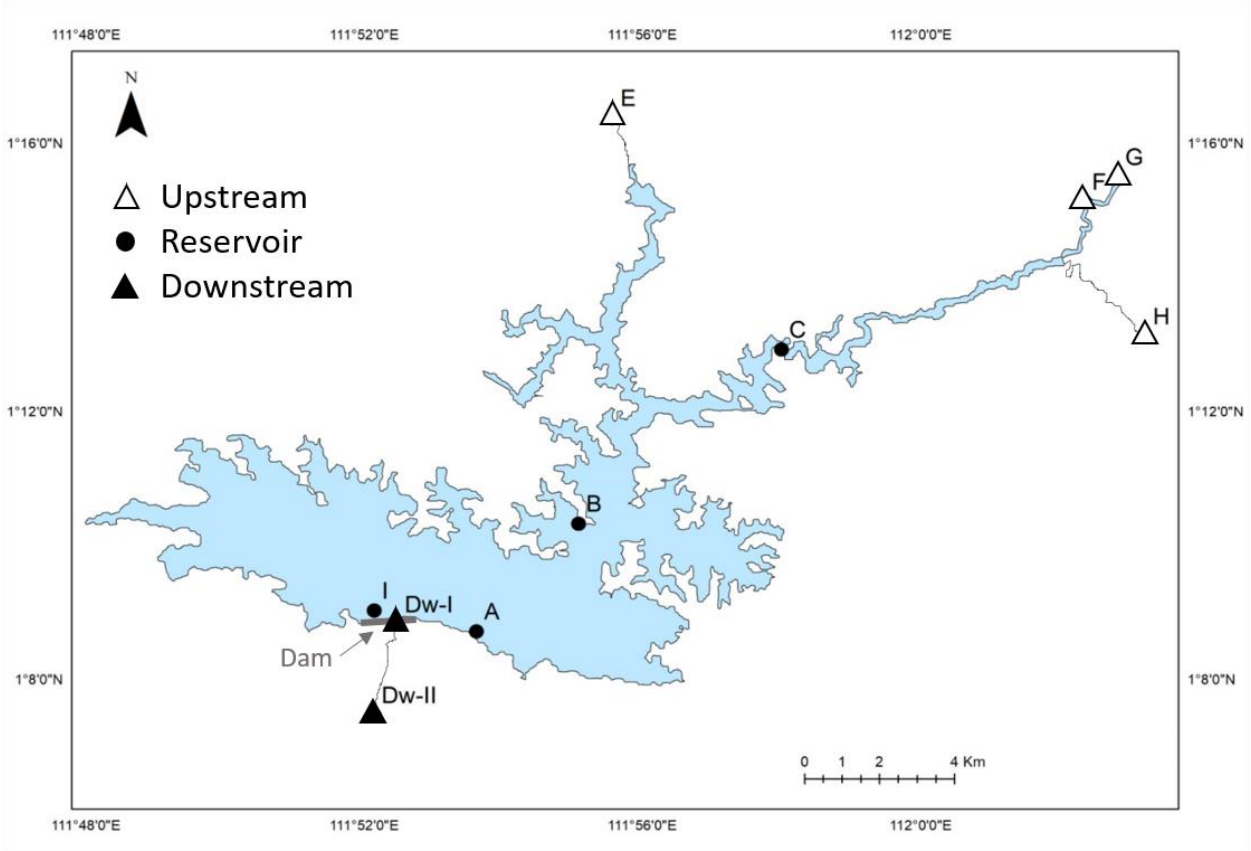

837

838 Figure 1

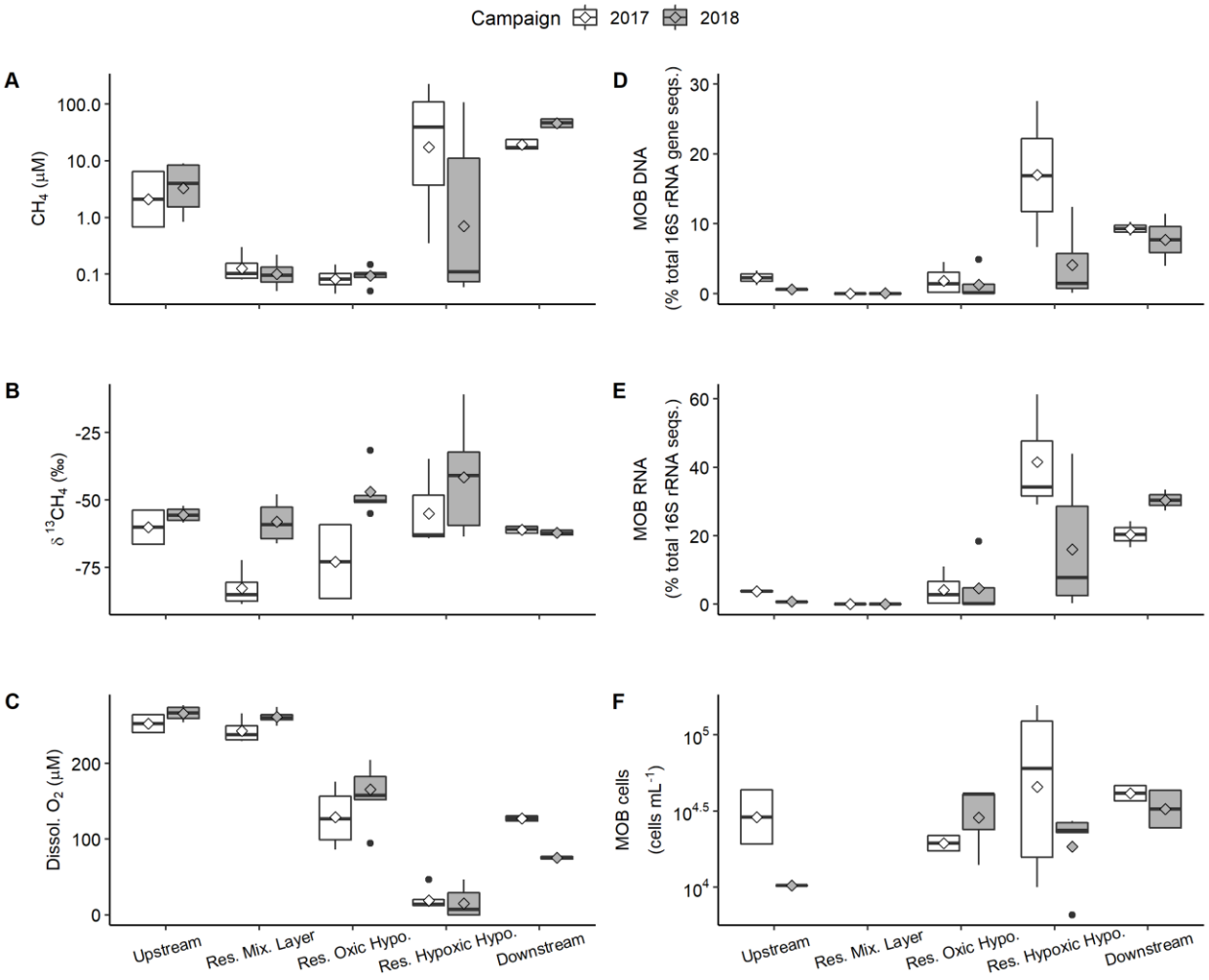

839

840 Figure 2

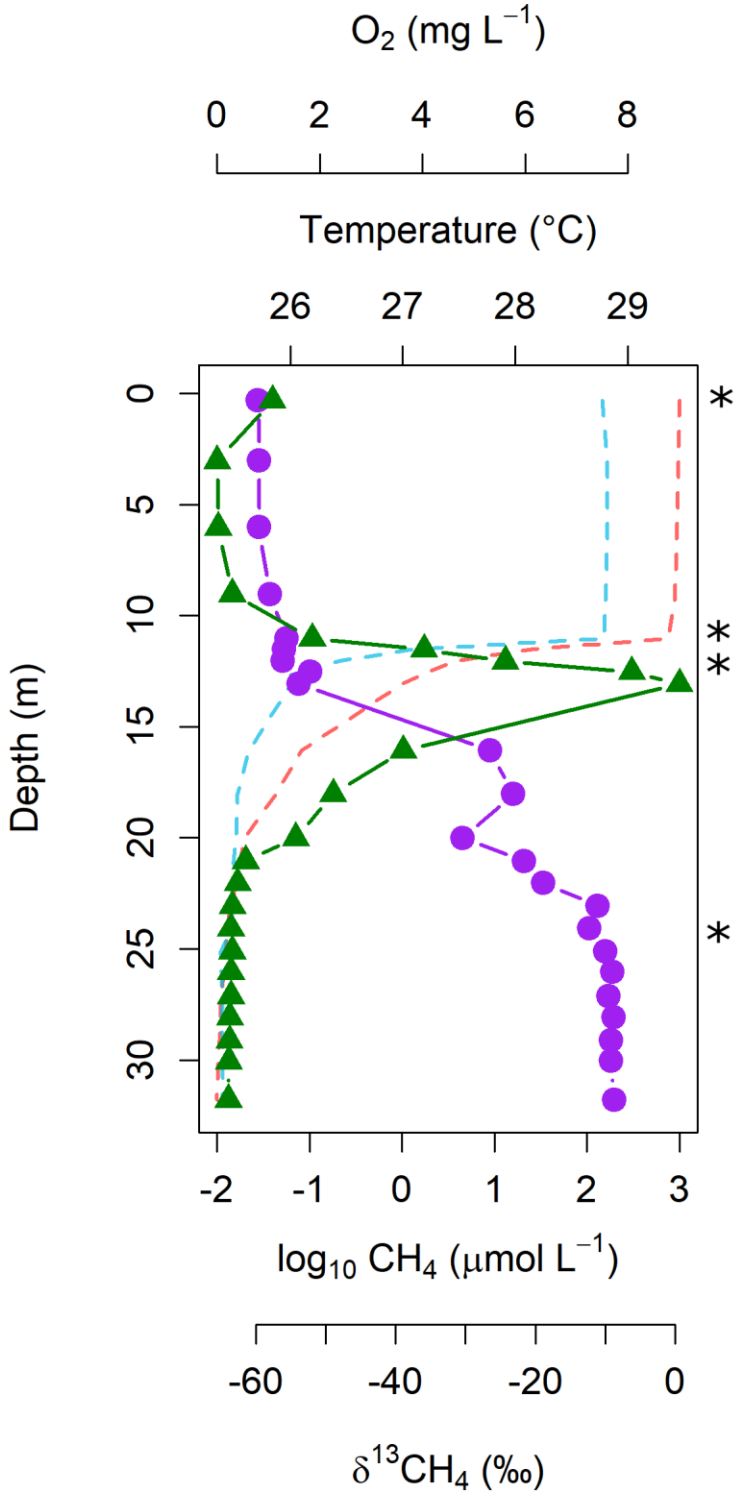

841

842 Figure 3

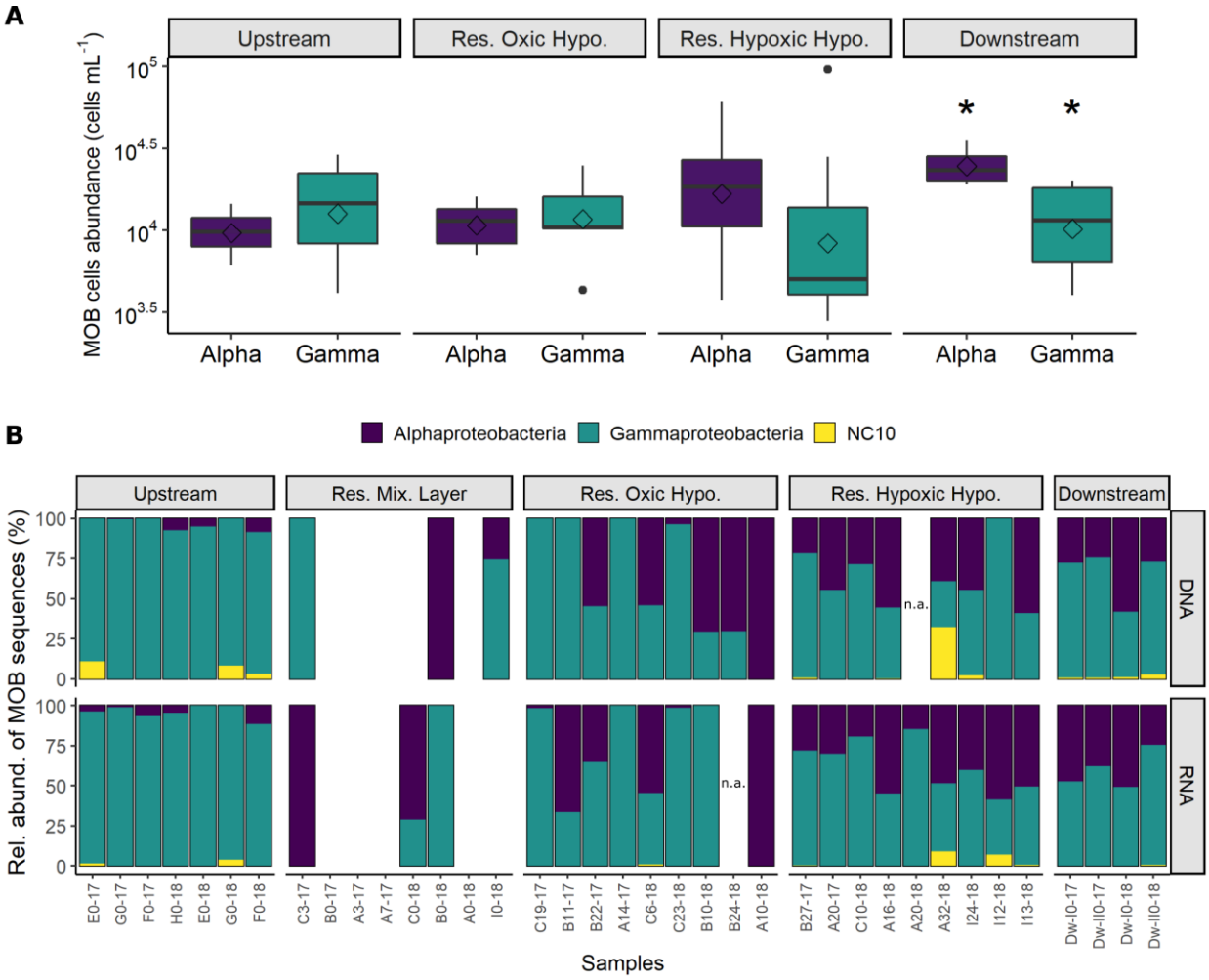

843

844 Figure 4

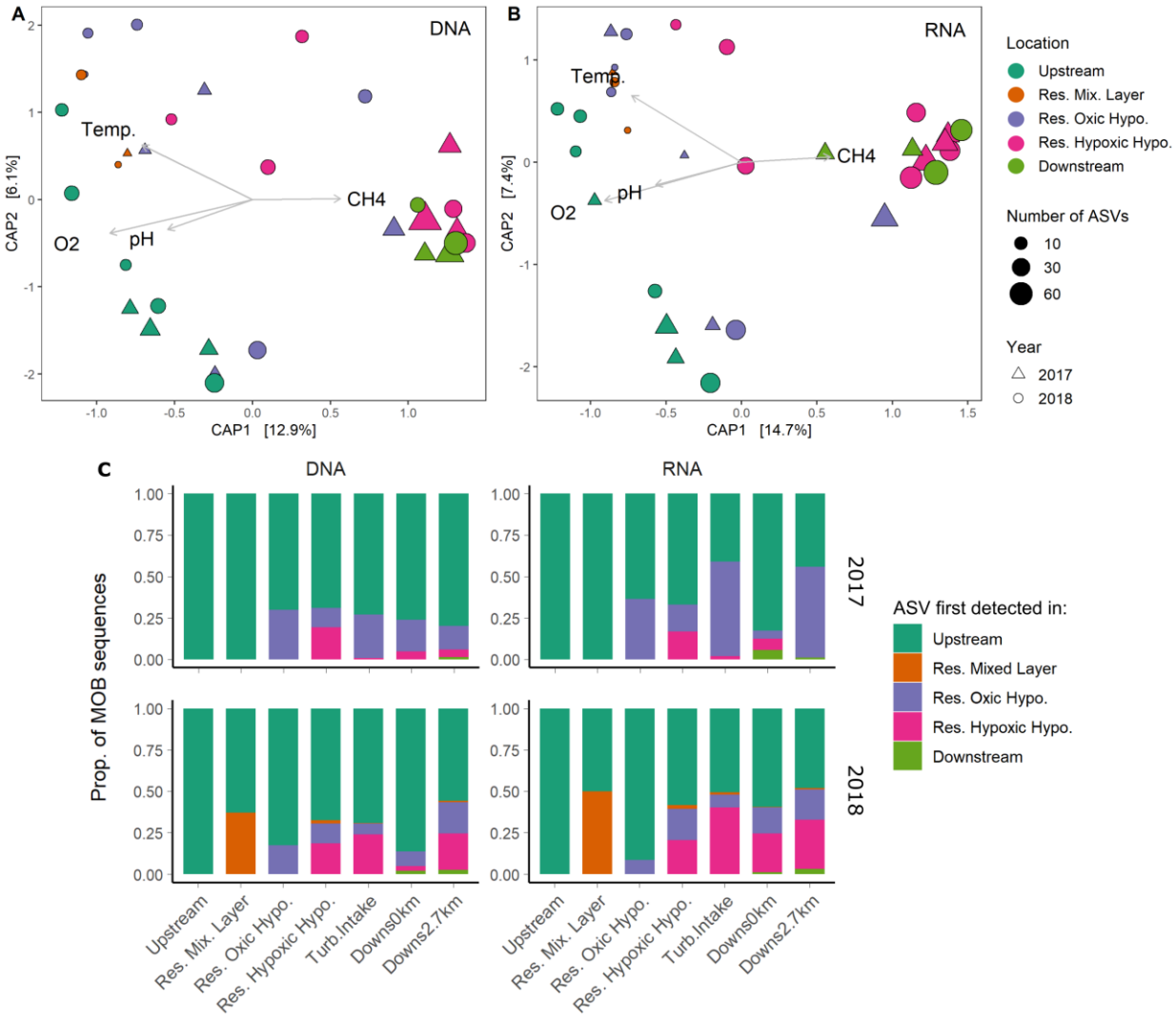

845

846 Figure 5

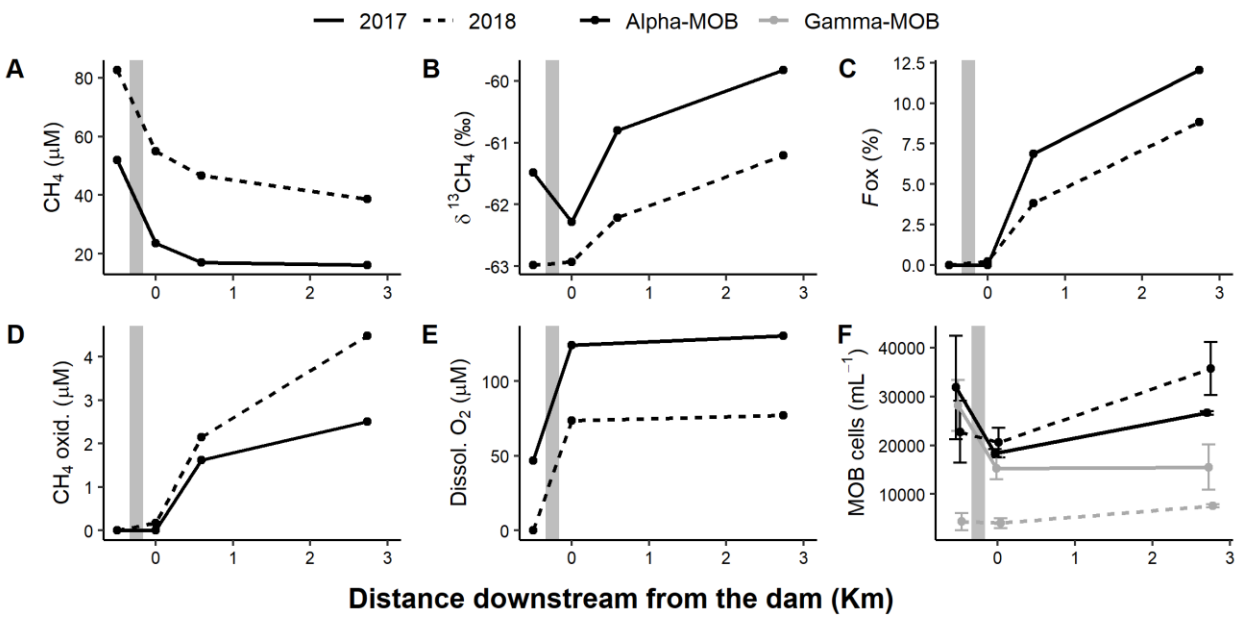

847

848 Figure 6